Altered energy transfer from mitochondria to sarcoplasmic reticulum after cytoarchitectural perturbations in mice hearts.

James R. Wilding, Frédéric Joubert, Carla de Araujo, Dominique Fortin, Marta Novotova, Vladimir Veksler, Renée Ventura-Clapier

ALTERED ENERGY TRANSFER FROM MITOCHONDRIA TO SARCOPLASMIC RETICULUM AFTER CYTOARCHITECTURAL PERTURBATIONS IN MICE HEARTS

Short title: Energy transfer depends on heart cytoarchitecture

James R. Wilding[1,2], Frédéric Joubert[1,2], Carla de Araujo[1,2], Dominique Fortin[1,2], Marta Novotova[3], Vladimir Veksler[1,2], Renée Ventura-Clapier[1,2]

[1] U-769 INSERM, Châtenay-Malabry, France

[2] University Paris-Sud 11, IFR 141, Faculty of Pharmacy, Châtenay-Malabry, France

[3] Institute of Molecular Physiology & Genetics, Slovak Academy of Sciences, Bratislava, Slovak Republic

Address for correspondance: Dr Renée Ventura-Clapier
U-769 INSERM
Faculté de Pharmacie
Université Paris-Sud
5 rue J-B Clément
92296 Châtenay-Malabry
France

Tel.: (33-1) 46.83.57.63.
Fax: (33-1) 46.83.54.75.
E-mail: renee.ventura@cep.u-psud.fr

Number of words: 4571

Abstract

Sarcoplasmic reticulum (SR) calcium pump function requires a high local ATP/ADP ratio, which can be maintained by direct nucleotide channeling from mitochondria, and by SR-bound creatine kinase (CK)-catalyzed phosphate-transfer from phosphocreatine. We hypothesized that SR calcium uptake supported by mitochondrial direct nucleotide channeling, but not bound CK, depends on the juxtaposition of these organelles. To test this, we studied a well-described model of cytoarchitectural disorganization, the muscle LIM protein (MLP)-null mouse heart. Subcellular organization was characterized using electron microscopy, and mitochondrial, SR and myofibrillar function were assessed in saponin-permeabilized fibers by measuring respiration rates and caffeine-induced tension transients. MLP-null hearts had fewer, less tightly-packed intermyofibrillar mitochondria, and more subsarcolemmal mitochondria. The apparent mitochondrial Km for ADP was significantly lower in MLP-null heart than control (175 ± 15 versus 270 ± 33 µM), indicating greater ADP accessibility, although maximal respiration rate, mitochondrial content and total CK activity were unaltered. MLP-null myofiber active tension was 54% lower than control (39 ± 3 versus 18 ± 1 mN/mm^2), consistent with cytoarchitectural disorganization. MLP-null fiber SR calcium loading was similar to that in control when energy support was provided via bound CK, but ~36% lower than controls when energy support was provided by mitochondria ($p<0.05$). Mitochondrial support for SR calcium uptake was also specifically decreased in desmin-null hearts, another model of cytoarchitectural perturbation. Thus, despite normal oxidative capacity, direct nucleotide channeling to the SR was impaired in MLP deficiency, concomitant with looser mitochondrial packing and increased nucleotide accessibility to this organelle. Changes in cytoarchitecture may therefore impair subcellular energy transfer and contribute to energetic and contractile dysfunction.

Introduction

Cardiomyocytes are a paradigm of highly compartmentalized cells. They possess a sophisticated subcellular architecture, in which repeated arrays of sarcomeres, T-tubules, sarcoplasmic reticulum (SR) and mitochondria interact, causing muscle contraction and relaxation. The coordinated production of calcium microdomains triggers contraction (Wang *et al.*, 2004), while myofibril-/SR-associated ATP pools provide the energy for cardiac function (Andrienko *et al.*, 2003). Helping maintain this cytoarchitecture is the cytoskeleton, which holds sarcomeres in lateral register, mechanically couples myofibrils of adjacent myocytes, and transduces mechanical stress signals (Fatkin & Graham, 2002). Cytoarchitectural perturbation may result from mutation or deletion of cytoskeletal genes such as muscle LIM protein (MLP) or desmin (Fatkin & Graham, 2002; Arber *et al.*, 1997; Kay *et al.*, 1997) and from hemodynamic overload, in which cardiac hypertrophy, changes in mitochondrial size, number and function, and cytoskeletal protein accumulation occur (Ventura-Clapier *et al.*, 2004; Tagawa *et al.*, 1998).

Cardiac muscle cytoarchitecture is also characterized by the spatial separation of energy-utilizing and producing sites (Dzeja *et al.*, 2000). The efficiency of contraction and relaxation depends on myofibrillar function and SR calcium uptake, respectively, and also on a high local ATP/ADP ratio maintained by a constant ATP supply to, and ADP withdrawal from, the myofibrillar and SR-calcium ATPases. Mitochondria produce most of the ATP in cardiac cells, but the simple diffusion of nucleotides between them and myofibrils/SR via the bulk cytosol cannot on its own sustain cardiac function, due to thermodynamic and kinetic limitations (Dzeja & Terzic, 2003). To solve this problem, cardiomyocytes use specialized systems of energy transfer such as creatine kinase (CK), which is bound to the mitochondrial inner membrane, myofibrils and SR and which efficiently transfers the high-energy

phosphate-group of mitochondrial ATP to ADP in the vicinity of the myofibrils and SR. Recently, we showed that mitochondria can directly support myofibrillar/SR-calcium ATPase function as efficiently as the bound CK-system, and much better than cytosolic ATP alone (Kaasik *et al.*, 2001). Consistent with this direct ATP channeling, others have shown that mitochondria can directly withdraw ADP from myofibrils/SR (Saks *et al.*, 2001).

As direct channeling of ATP from mitochondria to the SR depends on the interaction of these two organelles, we hypothesized that the process would be altered by perturbation of the arrangement of mitochondria with SR. To test this, we characterized energy transfer in MLP-null mouse hearts, which show myofibre disarray, disorganized mitochondria and cytoskeletal remodeling (Arber *et al.*, 1997; van den Bosch *et al.*, 2005; Wilding *et al.*, 2005) We found fewer, less tightly-packed intermyofibrillar mitochondria in this model, with more subsarcolemmal mitochondria. Concomitant with these changes, the accessibility of exogenous ADP to mitochondria was higher in MLP-null hearts. Using a method thoroughly worked-out in our laboratory, based on the use of tension measurements after SR calcium release with caffeine addition, we found that SR calcium loading by mitochondrial ATP-channeling was reduced, whereas loading supported by bound CK was similar to controls. To see whether our findings were specific to the MLP-deficient heart, we used a second model of cytoarchitectural perturbation, the desmin-null mouse heart, in which we also found impaired SR calcium loading supported by mitochondrial direct ATP channeling. We conclude that nucleotide channeling may depend on mitochondrial packing with the SR, such that cytoarchitectural perturbation could promote energetic dysfunction.

Materials and Methods

Animals

Two-to-three month old C57BL/6 mice (control), MLP-null mice (kind gift, Prof. Kieran Clarke, University of Oxford) and desmin-null mice (kind gift from Dr D. Paulin, Institut Pasteur) were anesthetized by intraperitoneal injection of sodium thiopental (150mg/kg). Hearts were excised and rinsed in ice-cold calcium-free Krebs solution equilibrated with 95% O_2/5% CO_2. For mitochondrial, SR and myofibrillar function measurements, papillary muscle fibers were dissected and permeabilized for 30 minutes in saponin (50 µg/mL) or Triton X-100 (1%), as described previously (Kaasik *et al.*, 2001; De Sousa *et al.*, 1999).

Electron microscopy

Left ventricular tissue was excised from control and MLP-null mouse hearts (n = 5, both groups), and fixed with 2% glutaraldehyde in cacodylate buffer (Na Cacodylate 150 mmol/L, $CaCl_2$ 2 mmol/L, pH 7.3). Tissue samples were postfixed in cacodylate buffer with 1% osmium tetroxide, contrasted with 1% uranyl acetate in H_2O, dehydrated, and embedded in Durcupan (Fluka Chemie AG, Sweden). Ultrathin longitudinal sections were stained with lead citrate and viewed using a JEM 1200 (JEOL, Japan) electron microscope. Images were recorded using a Gatan DualVision 300W CCD camera (Gatan Inc., Warrendale, PA, USA).

Mitochondrial function

Respiration rate and its sensitivity to ADP and creatine were measured in saponin-permeabilized control and MLP-null cardiac fibers using a Clark electrode (Strathkelvin Instruments), as described previously (Veksler *et al.*, 1995). We determined the basal rate of mitochondrial oxygen consumption in the absence of ADP, V_0, the maximal rate of oxygen consumption stimulated with 2 mmol/L ADP, V_{max}, the acceptor control ratio, V_{max}/V_0

(control n = 11, MLP-null n = 29), and the apparent Michaelis-Menten constant for ADP, Km(ADP) (control n = 8, MLP-null n = 20).

Myofibrillar intrinsic properties and estimation of SR calcium uptake

The intrinsic sensitivity of control and MLP-null (n = 8, both groups) myofibrils to calcium and ATP was measured in triton X-100-permeabilized cardiac fibers, as described previously (Ventura-Clapier *et al.*, 1995). SR calcium loading for 30 s, 60 s, 180 s and 300 s was measured in saponin-permeabilized control (n = 7-10) and MLP-null (n = 5-11) mouse cardiac fibers, and for 180 s in desmin-null fibers (n = 10) as described previously (Minajeva *et al.*, 1996; Kaasik *et al.*, 2001). Briefly, calcium uptake at pCa 6.5 (pCa is the negative logarithm of the free calcium concentration) occurred in the presence of exogenous ATP, with or without endogenous mitochondrial ATP production and/or CK-system activation. SR calcium release was elicited with 5 mmol/L caffeine, and was detected using the resulting contractile force transient. Despite using different energetic loading conditions, calcium release was always measured using the same solution, which provided exogenous ATP, mitochondrial and CK-system activation together. By relating the subsequent contractile force elicited with caffeine to the calcium-force curve for each fiber, the $[Ca^{2+}]$-time integral was calculated as an index of SR calcium load (for further details and discussion, see (Kaasik *et al.*, 2001; Minajeva *et al.*, 1996). The ATP channeling solution (ATP+MITO) contained (in mmol/L) ethylene glycol-bis(ß-aminoethyl ether)*N,N,N',N'*-tetra-acetic acid 10 (EGTA, 0.2 during calcium release), *N,N*-bis[2-hydroxyethyl]-2-aminoethanesulfonic acid 40 (BES, pH 7.1), free Mg^{2+} 1, taurine 10, glutamic acid 5, malic acid 2, K_2HPO_4 3, dithiothreitol 0.5, P^1,P^5 diadenosine pentaphosphate 0.04 (to inhibit adenylate kinase activity), ruthenium red 0.005 (to block mitochondrial calcium uptake), MgATP 3.16, ionic strength was adjusted to 160 mmol/L with potassium methanesulfonate, and 6% dextran was added to maintain

normal cell volume. Addition of 12 mmol/L phosphocreatine (PCr) to this solution caused SR loading by ATP channeling and the bound CK system together (ATP+Mito+CK, optimal energetic conditions), and when 2mM sodium azide was also present then mitochondrial respiration was blocked such that loading was by the CK system only (ATP+CK). Addition of 2mmol/L azide in the absence of PCr caused SR loading by exogenous ATP only (ATP).

Biochemical analysis

Activities of total CK, citrate synthase (CS) and mitochondrial complex I were measured using standard assays (Ventura-Clapier *et al.,* 1995; Veksler *et al.,* 1995; Wharton & Tzagoloff, 1967; Estornell *et al.*, 1993)

Statistics

Data are expressed as mean ± SEM. Statistical differences between two or more groups were determined by analysis of variance (ANOVA). Differences in SR loading by the same fiber under different energetic conditions were assessed by one-way ANOVA with repeated measures, using a Newman-Keuls. Significance was defined by a p-value less than 0.05 (95% confidence).

Results

Anatomy and cardiac cytoarchitecture in MLP-null mice

Compared with controls, heart and lung weights normalized to tibia length were increased in MLP-null mice by 36% and 20%, respectively (Table 1). Using electron microscopy, we confirmed that cardiac cytoarchitecture was greatly perturbed in MLP-null mice (Figures 1 and 2). In control heart, there was an orderly arrangement of myofibrils, interspersed by tightly-packed rows of mitochondria (Figure 1A,C). By contrast, MLP-null hearts had disorganized myofibrils with widened Z-lines, and intermyofibrillar mitochondria that were irregularly dispersed and not arranged in longitudinal columns (Figure 1B, D). Mitochondria, myofibrils and SR appeared to be less tightly packed in MLP-null tissue, with more cytosol visible, and the content of subsarcolemmal mitochondria was increased (Figure 1B,D). At intercalated disks, membrane folding was more elaborate in MLP-null heart than control, often with myofibrillar degeneration and an absence of mitochondria (Figure 2A-C). However, large mitochondrial aggregates were sometimes visible in other regions of MLP-null myocytes (Figure 2D), so that no obvious changes in total mitochondrial content were apparent.

Myofibrillar, mitochondrial and creatine kinase function

Myofibrillar function was assessed in permeabilized cardiac fibers from MLP-null and control mice (Table 2). Maximal active tension at pCa 4.5 was 54% lower in MLP-null mouse heart than control, consistent with myofibrillar disarray, whereas passive tension, calcium sensitivity and ATP sensitivity were unchanged. In order to determine the intrinsic activity of ATP-regenerating systems in MLP-null cardiac muscle, i.e. independently of SR- or myosin-ATPase function, we measured mitochondrial function *in situ* and total creatine kinase activity in heart tissue extracts (Table 2). The maximal rate of ADP-stimulated

mitochondrial respiration with glutamate and malate as electron donors, and total ADP-stimulated CK activity, were similar in control and MLP-null mice, suggesting that the intrinsic function of these two systems was normal. However, mitochondrial apparent Km(ADP) was 35% lower in MLP-null cardiac fibers than control (p < 0.05), indicating increased sensitivity to ADP. The basal, uncoupled respiration rate, V_0, was 28% lower in MLP-null fibers, and consequently the acceptor control ratio was 49% higher. Total citrate synthase and the activity of complex I of the respiratory chain were normal in MLP-null heart (Table 2), consistent with normal mitochondrial content and maximal respiration rate.

SR calcium uptake

In saponin-permeabilized control and MLP-null mouse cardiac fibers, we measured SR calcium loading over time, supported by mitochondrial direct ATP channeling and bound creatine kinase (Figures 3-5). The SR was loaded with calcium using different solutions that controlled the ATP source, and SR calcium content was assessed using the force transient induced by caffeine stimulation. Caffeine-induced tension transients had decreased amplitude in MLP-null cardiac fibers compared to control (Figure 3), consistent with reduced maximal active tension (Table 2). Using the force-calcium relationship for each fiber, developed tension was converted into calcium concentration units, and the resulting calcium concentration-time integral (SCa) was used as an index of SR calcium content. By this method, we found similar SR calcium content in control and MLP-null fibers after loading under optimal energetic conditions (ATP+Mito+CK, Figure 4A). It was clear that mitochondrial ATP channeling occurred in both control and MLP-null mouse fibers, because calcium uptake was much greater with ATP+Mito solution than with exogenous ATP alone (Figure 4 and 5). Compared with controls, SR calcium load supported by mitochondrial direct ATP channeling (ATP+Mito) was decreased by 37% and 35% in MLP-null fibers after 180 s

and 300 s of loading, respectively (p < 0.05, Figure 4B). Relative to controls, calcium loading supported by bound creatine kinase (ATP+CK) was normal in MLP-null fibers (Figure 4C), whereas loading supported by exogenous ATP alone was 54% higher after 300 s of loading (9.2 ± 0.9 versus 14.2 ± 1.7 µM.s) (Figure 4C and D). Note that after 5 min of calcium loading in control mice, there was a tendency to have lower calcium release in the presence of mitochondrial substrates relative to maximum loading capacity (ATP+MITO+CK), but this was not statistically significant (one-way ANOVA with repeated measures (Newman-Keuls) gives p = 0.19, n = 5)

In order to determine the relative ability of different energetic systems to support SR calcium loading, we compared the size of caffeine-induced calcium transients in the same fiber after 180 s of loading by each of the four conditions (Figure 5). In controls, SR calcium content was similar whether loading was supported by mitochondrial direct ATP channeling, by bound CK, or by both systems together, whereas loading with exogenous ATP alone was significantly lower compared with these conditions.

In MLP-null fibers, loading by mitochondrial direct ATP channeling (ATP+Mito) was 23% lower than loading by ATP+CK (p = 0.005), and 38% lower than loading by ATP+Mito+CK (p = 0.0001). Loading by bound creatine kinase (ATP+CK) was 20% lower than loading by ATP+Mito+CK in MLP-null fibers (p = 0.01), and loading with exogenous ATP alone was significantly lower than all other conditions. Similar results were obtained with both groups at 300 s loading (graphs not shown.

Relative SR calcium content after 180 s loading was also measured in desmin-null mouse cardiac fibers (Figure 5). Loading supported by ATP+Mito was 37% lower than loading by ATP+CK (p=0.03), and 46% lower than loading by ATP+Mito+CK (p=0.004), whereas

loading by bound creatine kinase (ATP+CK) was not significantly different from loading by ATP+Mito+CK. Like MLP-null hearts therefore, desmin-null fibers had reduced SR calcium content supported by mitochondrial direct ATP channeling.

These data reveal that in cardiac fibers lacking the cytoskeletal proteins MLP or desmin, energetic coupling of mitochondria with the sarcoplasmic/endoplasmic reticulum Ca^{2+} ATPase (SERCA) by direct nucleotide channeling was impaired, whereas energetic support by bound creatine kinase was near-normal.

Discussion

In this study, we used a model of subcellular disorganization, the MLP-null mouse heart, to determine the role cytoarchitecture plays in the direct transfer of energy from mitochondria to the SR calcium pump. Relative to controls, MLP-null hearts were characterized by 1) myofibrillar disorganization, looser packing of mitochondria with myofibrils and SR, and increased accessibility of exogenous ADP to mitochondria, 2) normal mitochondrial content and oxidative capacity and normal total creatine kinase activity, 3) impaired calcium uptake with mitochondrial direct ATP channeling, but near-normal calcium uptake when bound creatine kinase was active. Similarly impaired direct mitochondrial energy channeling was also observed in hearts lacking the cytoskeletal protein desmin. Therefore, perturbation of cardiac cytoarchitecture might impair direct energy transfer between mitochondria and SR.

MLP-null mice develop dilated cardiomyopathy between 4 and 8 weeks of age (Hoshijima *et al.*, 2002). In addition, rodent cardiomyocyte cytoarchitecture is not fully developed until 6-8 weeks of age, when physiological cardiomyocyte hypertrophy and energy flux compartmentation are complete (Hoerter *et al.*, 1994). Use of 2-3 month old MLP-null mice was therefore advantageous in that developmental changes in cytoarchitecture were complete and heart failure was not long established, so that oxidative capacity and creatine kinase activity were not yet decreased, and so changes in mitochondrial direct ATP channeling could be related to cytoarchitecural perturbation. In addition, to show that changes were not specifically related to MLP loss, but were most probably a consequence of cytoarchitectural disorganization, we used another genetic model of cytoarchitectural perturbation, the desmin-null mouse, and found similarly impaired mitochondrial direct ATP channeling.

Myofibrillar disarray with intercalated disk remodeling is a hallmark of MLP-null mouse cardiomyopathy (Arber *et al.*, 1997; Minamisawa *et al.*, 1999; Ehler *et al.*, 2001) as we confirmed using electron microscopy. Consistent with this phenotype, and shown here for the first time, we found lower maximal active tension in Triton-skinned cardiac fibers lacking MLP, although myofibrillar calcium and ATP sensitivities were unchanged. We also found increased cytosolic space in MLP-null hearts, as described previously (Arber *et al.*, 1997), concomitant with looser packing of mitochondria with SR and myofibrils. Van den Bosch and co-workers similarly reported misalignment of mitochondria with myofibrils in MLP-null mouse hearts, with reduced mitochondrial size and some regions lacking mitochondria altogether (van den Bosch *et al.*, 2005). Although we saw regions lacking mitochondria, and fewer intermyofibrilar mitochondria, we also observed areas with mitochondrial accumulation, and more subsarcolemmal mitochondria in MLP-null heart. This may reflect differences between MLP-null mouse colonies in the two studies, or different stages of cardiomyopathy, which is progressive in this model (Hongo *et al.*, 2000). Maximal glutamate/malate-stimulated respiration rate, complex I activity and citrate synthase levels were normal in our MLP-null hearts, therefore we conclude that at this stage, mitochondrial content and tissue oxidative capacity were normal, whereas the juxtaposition of mitochondria with SR and myofibrils was perturbed. It should be noted that we took care to assess mitochondrial function without disrupting the cellular structure so that our results reflect the true mitochondrial re/dis-organization. Thus, some rearrangement between both populations of mitochondria may have occurred. Such redistribution, despite maintained mitochondrial function within fibers, could result in diminished local mitochondria /SR crosstalk. Whatever the case, it emphasizes that subcellular organization is important for energetic regulation of SERCA, because a change in the distribution of functional mitochondria within cells alters local ATP/ADP ratio in the vicinity of SERCA.

MLP-null mouse heart mitochondria had a lower apparent Km(ADP) *in situ*, indicating increased sensitivity to stimulation by exogenous ADP. This is entirely consistent with looser mitochondrial packing and increased cytosolic space in these hearts, which would provide greater access of exogenous ADP to mitochondria. Conversely, we would expect the Km(ADP) for endogenous ADP produced by SERCA or myosin ATPase to be increased, since nucleotide channeling was impaired and mitochondria and SR appeared to be less tightly packed together in MLP-null hearts. This change in ADP sensitivity was therefore probably a consequence of cytoarchitectural perturbation. Alternatively, increased mitochondrial outer membrane permeability may underlie a decreased Km(ADP) (Saks *et al.*, 2003). Similar to MLP-deficient animals, mice lacking desmin had cardiomyopathy with a reduced mitochondrial Km(ADP) *in situ* and preserved oxidative capacity (Kay *et al.*, 1997), suggesting a similar pathophysiology in other models of cytoskeletal protein loss. Compared to controls, basal respiration rate was lower in MLP-null mouse cardiac fibers, causing a significant increase in the acceptor control ratio and suggesting reduced proton leak across the inner mitochondrial membrane. Since MLP may promote expression of uncoupling protein UCP3 (de Lange *et al.*, 2004), which is associated with dissipation of the proton gradient (Boehm *et al.*, 2001), it is possible that this was due to decreased UCP3 levels. Total ADP-stimulated creatine kinase activity was not significantly lower in MLP-null and control hearts, although it approached significance (p = 0.07). CK and mitochondrial function are decreased in other models of heart failure (De Sousa *et al.*, 1999), and may have decreased in our MLP-null hearts as the cardiomyopathy progressed.

To investigate direct interaction between organelles, we used a method that we initially developed 10 years ago (Minajeva *et al.*, 1996). It is based on the use of cardiac bundles

permeabilized with saponin in order to preserve integrity of the cellular architecture. It uses myofilaments as an internal probe for calcium released by SR. Maximal SR calcium uptake capacity is assessed by recording the tension time integral of the tension transient induced by caffeine at optimal and constant energy supply (ATP+Mito+CK). An advantage is that myofilaments respond to "the functional calcium". To circumvent possible confounding effects due to intrinsic myofibrillar changes in MLP (or desmin) deficiency and sensitization of myofilaments by caffeine , the calcium sensitivity of myofilaments was assessed for each fiber and released calcium was calculated from tension changes and calcium sensitivity (in the presence of caffeine to be in the same condition as during calcium release). Released calcium was thus calculated from tension changes and calcium sensitivity, which are equivalent to a calibration curve for each fiber (Minajeva *et al.*, 1996). An alternative possibility would have been to use recently developed SR-localized calcium indicator in order to monitor calcium loading. We tried to use two such indicators, Mag-Fluo4 and fluo-5N in mice hearts, but had great dificultly with the protocol. Both dyes appeared to saturate too soon during loading, and Mag-Fluo4 revealed itself to be highly susceptible to bleaching. Others have also reported specific difficulties with SR loaded fluorescent dyes in rodent myocytes (Venetucci *et al.*, 2003). Another alternative to our approach would have been to measure SR calcium release using fluorescent indicators located in the external medium. It is clear that there are also technical problems to overcome and that it requires expertise. In addition, most of the fluorescent dyes also interact with caffeine thus altering calcium measurements (Muschol *et al.*, 1999). Nevertheless, we believe that both approaches would provide similar results. Indeed, using permeabilized fibres, we could show the importance of local ATP/ADP ratios for optimal functioning of ATPases either by bound creatine kinase (Minajeva *et al.*, 1996) or by close energetic interactions between subcellular organelles (Kaasik *et al.*, 2001). These results have been confirmed and extended by others using

fluorescent dyes (Duke & Steele, 1999; Yang & Steele, 2002) and biochemical (Saks *et al.*, 2001) approaches.

To determine the effects of cytoarchitectural perturbation on mitochondrial direct ATP channeling, we compared SR calcium uptake supported by mitochondria, bound creatine kinase and exogenous ATP in permeabilized control and MLP-null mouse cardiac fibers. Previous studies have shown normal SERCA2 and phospholamban levels in MLP deficiency (Minamisawa *et al.*, 1999; Lorenzen-Schmidt *et al.*, 2005), and we now report normal SR calcium loading under optimal energetic conditions (ATP+Mito+CK), consistent with this. However, we found a defect in mitochondrial direct ATP supply (ATP+Mito) to the sarcoplasmic reticulum in MLP deficiency, which was not related to changes in the intrinsic oxidative capacity of mitochondria or a specific limitation in SERCA activity. In desmin-null hearts, we found a specific defect in the support for SR calcium uptake by mitochondrial direct ATP channeling, suggesting that this process may be impaired in many models of cytoskeletal protein loss and cytoarchitectural perturbation. Loading supported by bound-CK (ATP+CK) was slightly depressed in MLP-null fibers relative to loading under optimal energetic conditions, consistent with the tendency towards lower total CK activity in this model. With exogenous ATP only, SR calcium content in MLP-null fibers was significantly higher than in controls after 5 minutes of loading, consistent with increased nucleotide accessibility to intracellular organelles.

The main finding of this work is that muscle cytoarchitecture may play an important role in myofibrillar, SR and mitochondrial function and in direct channeling of ADP from the SR to mitochondria. It was already shown that myofibrillar disarray in cardiomyopathic hearts, for example, is associated with reduced contractile function (Arber *et al.*, 1997; McConnell *et al.*, 1999), while remodeling of the SR/T-tubule junction may underlie decreased excitation-

contraction coupling gain in heart failure (Gomez *et al.*, 2001). Others have shown that cytoskeletal proteolysis increased the rate of ADP diffusion and the sensitivity of mitochondrial respiration to ADP stimulation, concomitant with reduced ADP channeling from myofibrils/SR to mitochondria (Saks *et al.*, 2003). Previously, we showed that loss of mitochondrial and cytosolic creatine kinase caused compensatory remodeling of cytoarchitecture in cardiac and skeletal muscle, characterized by greater packing of mitochondria with myofibrils and SR, concomitant with maintained calcium uptake supported by mitochondrial direct ATP channeling (Kaasik *et al.*, 2001; Kaasik *et al.*, 2003). Recently it was suggested that muscle cytoarchitecture is organized around the 'intracellular energetic unit' (ICEU), consisting of a sarcomere coupled with a mitochondrion, SR and two T-tubules, which promotes nucleotide channeling and efficient communication between mitochondria, SR and sarcomeres (Saks *et al.*, 2001). Our electron microscopy images reveal disrupted ICEUs in MLP deficiency, which were associated with impaired mitochondrial direct ATP channeling to the SR, thus underlining the importance of muscle cytoarchitecture in energy transfer.

In this study we show that independent of changes of the energy-producing systems, cytoarchitectural changes can also affect the energetic support for calcium uptake. Calcium transient amplitude is decreased in MLP-deficient mouse cardiomyocytes and relaxation is slower in MLP-null mouse heart (Minamisawa *et al.*, 1999; Esposito *et al.*, 2000), perhaps partly due to impaired direct nucleotide channeling between mitochondria and SR (van den Bosch *et al.*, 2005). This may be especially important under conditions of increased workload, in which energy supply could become limiting. Interestingly, correction of the calcium cycling defect in MLP-null mice by phospholamban gene deletion also corrected the cytoarchitectural changes, suggesting that impaired calcium handling and the resulting

hemodynamic stress may themselves engender cytoarchitectural disorganization (Minamisawa *et al.*, 1999).

In summary, we have shown that in two models of cytoarchitectural perturbation and heart failure, MLP-null and desmin-null mouse hearts, there was a specific decrease in SR calcium loading supported by mitochondrial direct ATP channeling, with near-normal loading supported by bound creatine kinase. Cardiac cytoarchitecture is therefore optimized both for force production and efficient energy transfer, such that cytoarchitectural perturbation may impair mitochondrial direct ATP channeling and contribute to energy wastage and contractile dysfunction.

References

Andrienko, T., Kuznetsov, A.V., Kaambre, T., Usson, Y., Orosco, A., Appaix, F., Tiivel, T., Sikk, P., Vendelin, M., Margreiter, R. & Saks, V.A. (2003). Metabolic consequences of functional complexes of mitochondria, myofibrils and sarcoplasmic reticulum in muscle cells. *J Exp Biol* **206**, 2059-2072.

Arber, S., Hunter, J.J., Ross, J.Jr., Hongo, M., Sansig, G., Borg, J., Perriard, J.C., Chien, K.R. & Caroni, P. (1997). MLP-deficient mice exhibit a disruption of cardiac cytoarchitectural organization, dilated cardiomyopathy, and heart failure. *Cell* **88**, 393-403.

Boehm, E.A., Jones, B.E., Radda, G.K., Veech, R.L. & Clarke, K. (2001). Increased uncoupling proteins and decreased efficiency in palmitate-perfused hyperthyroid rat heart. *Am J Physiol Heart Circ Physiol* **280**, H977-83.

de Lange, P., Ragni, M., Silvestri, E., Moreno, M., Schiavo, L., Lombardi, A., Farina, P., Feola, A., Goglia, F. & Lanni, A. (2004). Combined cDNA array/RT-PCR analysis of gene expression profile in rat gastrocnemius muscle: relation to its adaptive function in energy metabolism during fasting . *FASEB J* **18**, 350-352.

De Sousa, E., Veksler, V., Minajeva, A., Kaasik, A., Mateo, P., Mayoux, E., Hoerter, J., Bigard, X., Serrurier, B. & Ventura-Clapier, R. (1999). Subcellular creatine kinase alterations. Implications in heart failure. *Circ Res* **85**, 68-76.

Duke, A.M. & Steele, D.S. (1999). Effects of creatine phosphate on Ca2+ regulation by the sarcoplasmic reticulum in mechanically skinned rat skeletal muscle fibres. *J Physiol* **517** (Pt 2), 447-58.

Dzeja, P.P., Redfield, M.M., Burnett, J.C. & Terzic, A. (2000). Failing energetics in failing hearts. *Curr Cardiol Rep* **2**, 212-217.

Dzeja, P.P. & Terzic, A. (2003). Phosphotransfer networks and cellular energetics. *J Exp Biol* **206**, 2039-2047.

Ehler, E., Horowits, R., Zuppinger, C., Price, R.L., Perriard, E., Leu, M., Caroni, P., Sussman, M., Eppenberger, H.M. & Perriard, J.C. (2001). Alterations at the intercalated disk associated with the absence of muscle LIM protein. *J Cell Biol* **153**, 763-772.

Esposito, G., Santana, L.F., Dilly, K., Cruz, J.D., Mao, L., Lederer, W.J. & Rockman, H.A. (2000). Cellular and functional defects in a mouse model of heart failure. *Am J Physiol Heart Circ Physiol* **279**, H3101-H3112

Estornell, E., Fato, R., Pallotti, F. & Lenaz, G. (1993). Assay conditions for the mitochondrial NADH:coenzyme Q oxidoreductase. *FEBS Lett* **332**, 127-31.

Fatkin, D. & Graham, R.M. (2002). Molecular mechanisms of inherited cardiomyopathies. *Physiol Rev* **82**, 945-980.

Gomez, A.M., Guatimosim, S., Dilly, K.W., Vassort, G. & Lederer, W.J. (2001). Heart failure after myocardial infarction: altered excitation-contraction coupling.

Circulation **104**, 688-693.

Hoerter, J.A., Ventura-Clapier, R. & Kuznetsov, A. (1994). Compartmentation of creatine kinases during perinatal development of mammalian heart. *Mol Cell Biochem* 133-134, 277-86.

Hongo, M., Ryoke, T., Schoenfeld, J., Hunter, J., Dalton, N., Clark, R., Lowe, D., Chien, K. & Ross, J. Jr (2000). Effects of growth hormone on cardiac dysfunction and gene expression in genetic murine dilated cardiomyopathy. *Basic Res Cardiol* **95**, 431-441.

Hoshijima, M., Pashmforoush, M., Knoll, R. & Chien, K.R. (2002). The MLP family of cytoskeletal Z disc proteins and dilated cardiomyopathy: a stress pathway model for heart failure progression. *Cold Spring Harb Symp Quant Biol* **67**, 399-408.

Kaasik, A., Veksler, V., Boehm, E., Novotova, M., Minajeva, A. & Ventura-Clapier, R. (2001). Energetic crosstalk between organelles: architectural integration of energy production and utilization. *Circ Res* **89**, 153-159.

Kaasik, A., Veksler, V., Boehm, E., Novotova, M. & Ventura-Clapier, R. (2003). From energy store to energy flux: a study in creatine kinase-deficient fast skeletal muscle. *FASEB J* **17**, 708-710.

Kay, L., Li, Z., Mericskay, M., Olivares, J., Tranqui, L., Fontaine, E., Tiivel, T., Sikk, P., Kaambre, T., Samuel, J.L., Rappaport, L., Usson, Y., Leverve, X., Paulin, D. & Saks, V.A. (1997). Study of regulation of mitochondrial respiration in vivo. An analysis of influence of ADP diffusion and possible role of cytoskeleton. *Biochim Biophys Acta* **1322**, 41-59.

Lorenzen-Schmidt, I., Stuyvers, B.D., Ter Keurs, H.E., Date, M.O., Hoshijima, M., Chien, K.R., McCulloch, A.D. & Omens, J.H. (2005). Young MLP deficient mice show diastolic dysfunction before the onset of dilated cardiomyopathy. *J Mol Cell Cardiol* **39**, 241-250.

McConnell, B.K., Jones, K.A., Fatkin, D., Arroyo, L.H., Lee, R.T., Aristizabal, O., Turnbull, D.H., Georgakopoulos, D., Kass, D., Bond, M., Niimura, H., Schoen, F.J., Conner, D., Fischman, D.A., Seidman, C.E. & Seidman, J.G. (1999). Dilated cardiomyopathy in homozygous myosin-binding protein-C mutant mice. *J Clin Invest* **104**, 1235-1244.

Minajeva, A., Ventura-Clapier, R. & Veksler, V. (1996). Ca2+ uptake by cardiac sarcoplasmic reticulum ATPase in situ strongly depends on bound creatine kinase. *Pflugers Arch* **432**, 904-12.

Minamisawa, S., Hoshijima, M., Chu, G., Ward, C.A., Frank, K., Gu, Y., Martone, M.E., Wang, Y., Ross, J.Jr., Kranias, E.G., Giles, W.R. & Chien, K.R. (1999). Chronic phospholamban-sarcoplasmic reticulum calcium ATPase interaction is the critical calcium cycling defect in dilated cardiomyopathy. *Cell* **99** , 313-322.

Muschol, M., Dasgupta, B.R. & Salzberg, B.M. (1999). Caffeine interaction with fluorescent calcium indicator dyes. *Biophys-J* **77**, 577-86.

Saks, V., Kuznetsov, A., Andrienko, T., Usson, Y., Appaix, F., Guerrero, K., Kaambre, T.,

Sikk, P., Lemba, M. & Vendelin, M. (2003). Heterogeneity of ADP diffusion and regulation of respiration in cardiac cells. *Biophys J* **84**, 3436-3456.

Saks, V.A., Kaambre, T., Sikk, P., Eimre, M., Orlova, E., Paju, K., Piirsoo, A., Appaix, F., Kay, L., Regitz-Zagrosek, V., Fleck, E. & Seppet, E. (2001a). Intracellular energetic units in red muscle cells. *Biochem J* **356**, 643-57.

Tagawa, H., Koide, M., Sato, H., Zile, M.R., Carabello, B.A. & Cooper, G. 4th (1998). Cytoskeletal role in the transition from compensated to decompensated hypertrophy during adult canine left ventricular pressure overloading. *Circ Res* **82**, 751-761.

van den Bosch, B.J., van den Burg, C.M., Schoonderwoerd, K., Lindsey, P.J., Scholte, H.R., de Coo, R.F., van Rooij, E., Rockman, H.A., Doevendans, P.A. & Smeets, H.J. (2005). Regional absence of mitochondria causing energy depletion in the myocardium of muscle LIM protein knockout mice. *Cardiovasc Res* **65**, 411-418.

Veksler, V.I., Kuznetsov, A.V., Anflous, K., Mateo, P., van Deursen, J., Wieringa, B. & Ventura-Clapier, R. (1995). Muscle creatine kinase-deficient mice. II. Cardiac and skeletal muscles exhibit tissue-specific adaptation of the mitochondrial function. *J Biol Chem* **270**, 19921-19929.

Venetucci, L., Trafford, A.W. & Eisner, D.A. (2003). Illuminating sarcoplasmic reticulum calcium. *Circ-Res* **93**, 4-5.

Ventura-Clapier, R., Garnier, A. & Veksler, V. (2004). Energy metabolism in heart failure. *J Physiol* **555**, 1-13.

Ventura-Clapier, R., Kuznetsov, A.V., d'Albis, A., van Deursen, J., Wieringa, B. & Veksler, V.I. (1995). Muscle creatine kinase-deficient mice. I. Alterations in myofibrillar function. *J Biol Chem* **270**, 19914-19920.

Wang, S.Q., Wei, C., Zhao, G., Brochet, D.X., Shen, J., Song, L.S., Wang, W., Yang, D. & Cheng, H. (2004). Imaging microdomain Ca2+ in muscle cells. *Circ Res* **94**, 1011-1022.

Wharton, D.C. & Tzagoloff, A. (1967). Cytochrome oxidase from beef heart mitochondria. *Meth Enymol* **10**, 245-250.(Abstract)

Wilding, J.R., Schneider, J.E., Sang, A.E., Davies, K.E., Neubauer, S. & Clarke, K. (2005). Dystrophin- and MLP-deficient mouse hearts: marked differences in morphology and function, but similar accumulation of cytoskeletal proteins. *FASEB J* **19**, 79-81.

Yang, Z. & Steele, D.S. (2002). Effects of phosphocreatine on SR Ca(2+) regulation in isolated saponin-permeabilized rat cardiac myocytes. *J-Physiol* **539**, 767-77.

Acknowledgments

Table 1. Anatomical parameters in MLP-null mice.

	Con	MLP-null
Age (days)	77 ± 3	74 ± 2
Body wt (g)	26.3 ± 0.4	26.1 ± 0.5
Tibia length (mm)	17.7 ± 0.1	17.4 ± 0.4
Heart wt / tibia length (mg/mm)	7.4 ± 0.2	10.1 ± 0.5 **
Lung wt / tibia length (mg/mm)	7.9 ± 0.2	9.5 ± 0.6 *

* $p < 0.05$, ** $p < 0.0001$ vs. Con

Table 2. Organellar function and enzyme activities.

	Con	MLP-null
Myofibrillar function		
Active tension (mN/mm^2)	39 ± 3	18 ± 1 **
Resting tension (mN/mm^2)	2.6 ± 0.4	3.1 ± 0.3
pCa$_{50}$	5.71 ± 0.02	5.67 ± 0.01
pATP$_{50}$	3.24 ± 0.04	3.29 ± 0.04
Mitochondrial function		
V$_o$, µmol O$_2$/min/g dw	6.0 ± 0.4	4.3 ± 0.2 *
V$_{max}$, µmol O$_2$/min/g dw	22.5 ± 1.1	23.3 ± 1.0
Acceptor control ratio	3.9 ± 0.3	5.8 ± 0.3 **
Apparent Km(ADP)	270 ± 34	175 ± 15 *
Enzyme activities		
Total CK (IU/g protein)	4226 ± 385	3134 ± 365
CS (IU/g protein)	942 ± 112	923 ± 67
Complex I (IU/g protein)	933 ± 47	898 ± 88

*p<0.05, **p<0.005 vs. Con

Figure Legends

Figure 1. Electron microscopic images of left ventricle from control (A, C) and MLP-null (B,D) mice. (A) Overview of a control myocyte in longitudinal section, with mitochondria arranged in longitudinal columns. (B) Overview of an MLP-null cardiomyocyte, showing myofibrillar disorganization, an irregular arrangement of intermyofibrillar mitochondria, and increased content of subsarcolemmal mitochondria. (C) Detail of sarcomeres in a control myocyte, showing mitochondria tightly packed with SR. (D) Detail of sarcomeres in an MLP–null myocyte, showing looser packing of mitochondria with SR, irregular and widened Z lines, and cytoplasm in the intermyofibrillar space. Arrowheads show mitochondria, arrows show SR.

Figure 2. Electron microscopic images of intercalated disks in control (A) and MLP-null mouse heart (B,C), and of mitochondrial aggregates in MLP-null myocytes (D). (A) Longitudinal section of control myocyte showing myofibrils attached to the intercalated disc. (B) An oblique section through the widely spread intercalated disc of an MLP-null myocyte. (C) A longitudinal section through a region of intercalated disc lacking myofibrils in an MLP-null myocyte. (D) Mitochondrial aggregates in MLP-null myocytes.

Figure 3. Representative tension transients during SR calcium release in control (A) and MLP-null (B) cardiac fibers. The SR was loaded with calcium for 3 min in permeabilized fibers under different energetic conditions (ATP+Mito+CK, ATP+Mito, ATP+CK, ATP, see Methods), and then calcium load was estimated by relating these tension transients, elicited by caffeine stimulation, to the calcium-tension curve for each fiber.

Figure 4. SR calcium loading over time under different energetic conditions in control and MLP-null mouse cardiac fibers. SR calcium load was estimated using the surface of the tension transient caused by caffeine stimulation (S Ca). Energy supplied by exogenous ATP, mitochondria and the creatine kinase reaction (ATP+CK+Mito, panel A), by exogenous ATP and mitochondria (ATP+Mito, panel B), by exogenous ATP and creatine kinase (ATP+CK, panel C) and by exogenous ATP only (ATP, panel D). * $p < 0.05$ vs Con

Figure 5. Relative SR calcium content after 180 s loading, as a proportion of the load effected by ATP+Mito+CK in the same fiber, under different energetic conditions in control, MLP-null and desmin-null cardiac fibers. * $p < 0.05$ vs. ATP+Mito+CK, † $p < 0.05$ vs. ATP+CK, ‡ $p < 0.05$ vs. ATP+Mito. See Results section for precise p-values.
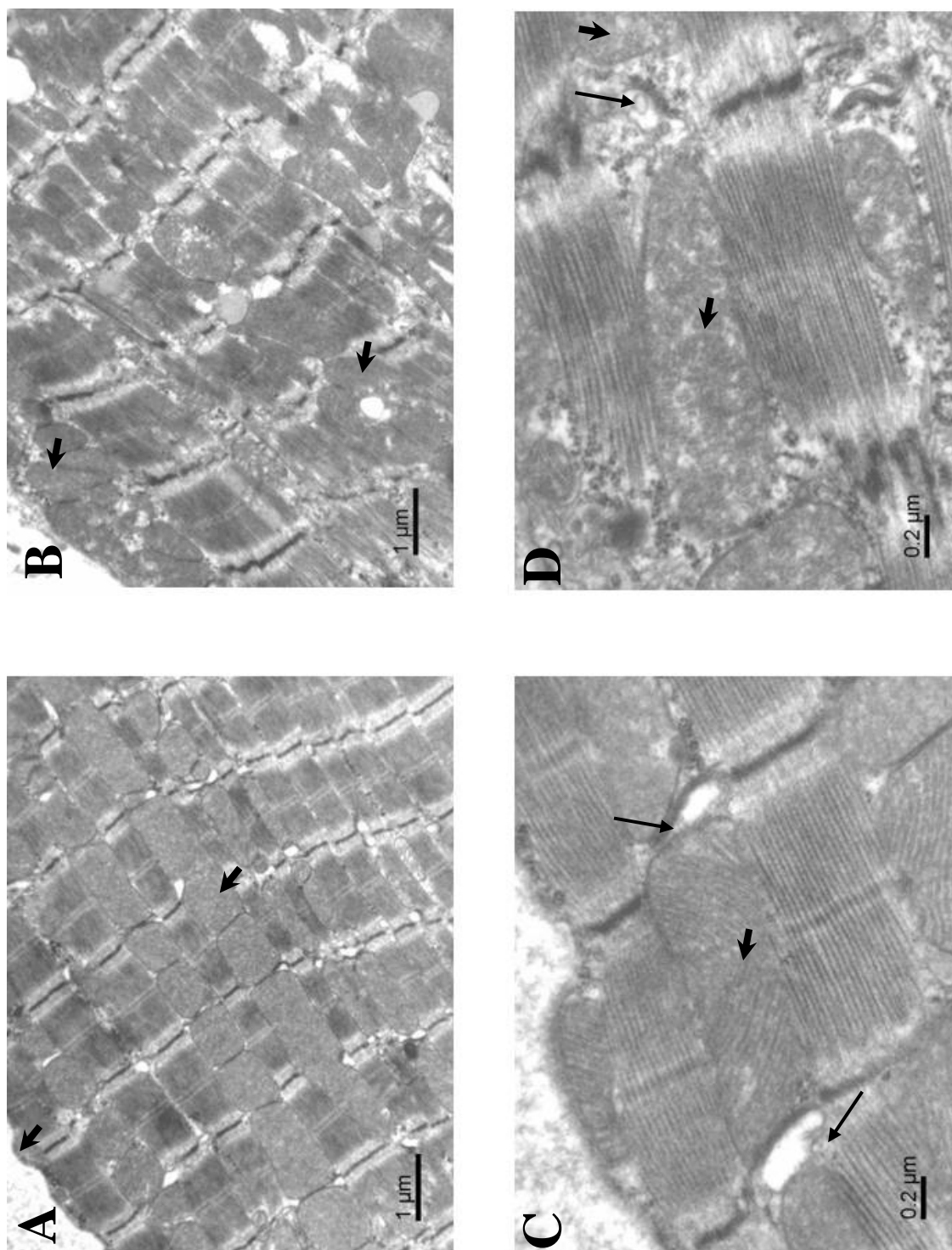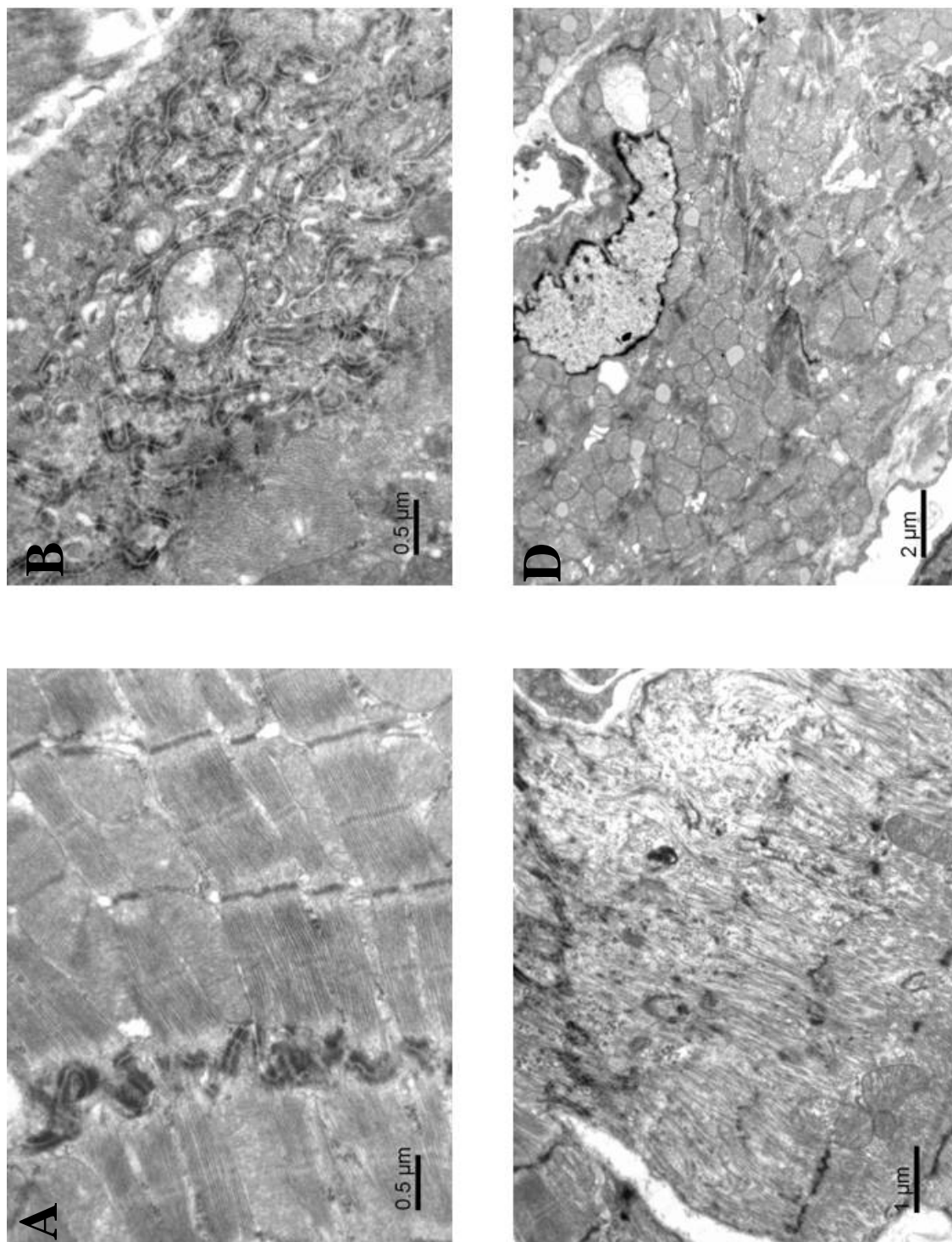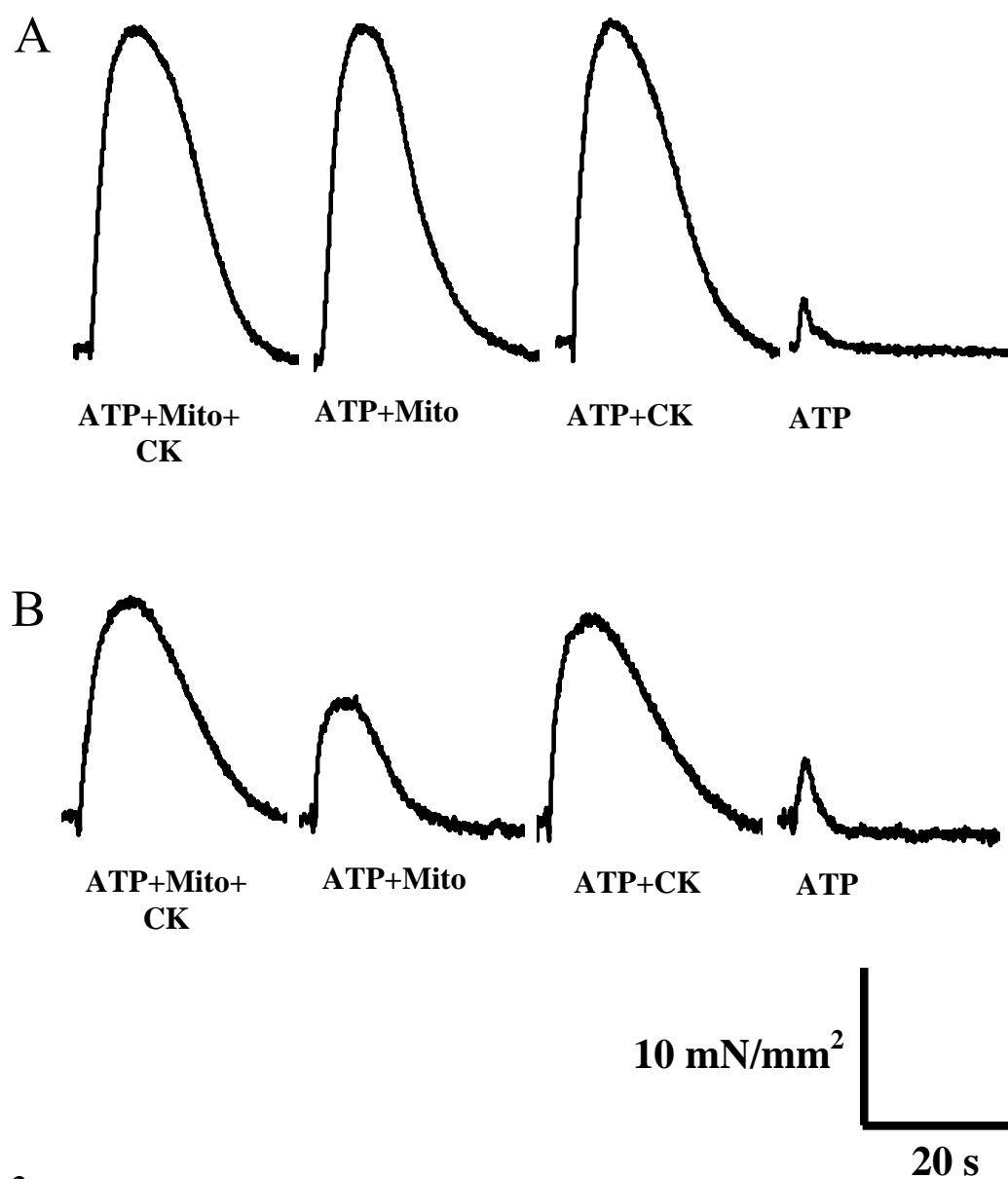
Figure 1.

Figure 2.
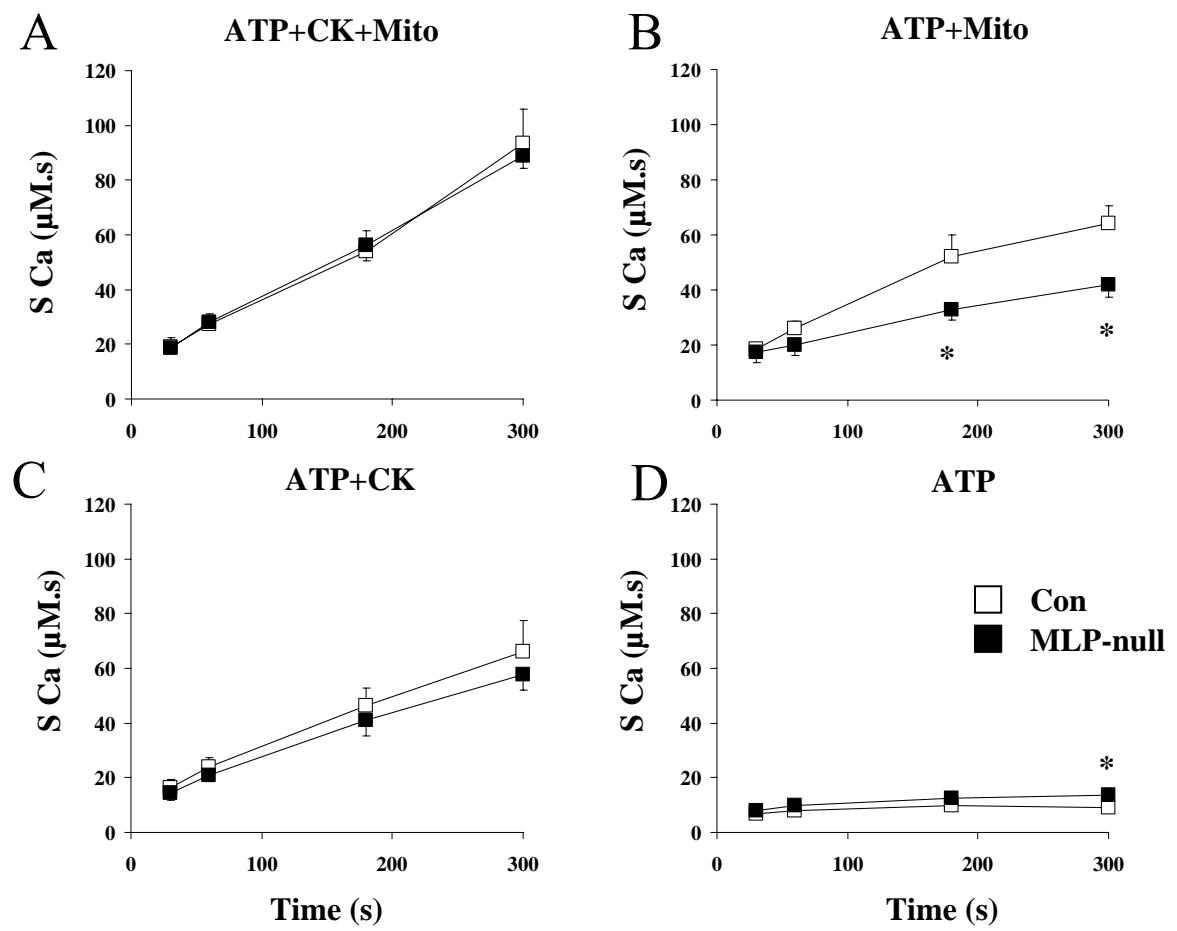
Figure 3.

Figure 4.

Figure 5.